Human brain distinctiveness based on EEG spectral coherence connectivity

Daria La Rocca, Patrizio Campisi, Balazs Vegso, Peter Cserti, Gyorgy Kozmann, Fabio Babiloni,
Fabrizio De Vico Fallani.

Abstract—The use of EEG biometrics, for the purpose of automatic people recognition, has received increasing attention in the recent years. Most of current analysis rely on the extraction of features characterizing the activity of single brain regions, like power-spectrum estimates, thus neglecting possible temporal dependencies between the generated EEG signals. However, important physiological information can be extracted from the way different brain regions are functionally coupled. In this study, we propose a novel approach that fuses spectral coherence-based connectivity between different brain regions as a possibly viable biometric feature. The proposed approach is tested on a large dataset of subjects (N=108) during eyes-closed (EC) and eyes-open (EO) resting state conditions. The obtained recognition performances show that using brain connectivity leads to higher distinctiveness with respect to power-spectrum measurements, in both the experimental conditions. Notably, a 100% recognition accuracy is obtained in EC and EO when integrating functional connectivity between regions in the frontal lobe, while a lower 97.41% is obtained in EC (96.26% in EO) when fusing power spectrum information from centro-parietal regions. Taken together, these results suggest that functional connectivity patterns represent effective features for improving EEG-based biometric systems.

Index Terms—EEG, Resting state, Biometrics, Spectral coherence, Match score fusion.

I. INTRODUCTION

ELECTROENCEPHALOGRAPHY (EEG) signals provide relevant information about individual differences related to brain anatomical and functional traits as already pointed out in early neurophysiologic studies [1], [2]. Although some isolated attempts to discriminate people from their electrical brain activity have been performed in the past [3] only recently the scientific community has started a more systematic investigation on the use of EEG signals as human distinctive traits which can be potentially used in a biometric system [4]. A variety of EEG elicitation protocols for the purpose of automatic user recognition have been implemented, ranging from resting states with eyes open (EO) and eyes closed (EC) to self-paced mental imagery [5].

In particular, resting states are advantageous conditions for biometric applications since they don't require active involvement of the subject during the EEG recording, thus reducing inconvenience, fatigue and artifact occurrences. From a neurophysiological perspective, ongoing EEG activity during resting states elicits patterns of synchronous oscillations in specific frequency ranges (from 1 to 40 Hz) that share and support basic cognitive functions [6]. Furthermore it has been suggested that EEG activity during resting wakefulness carries genetic information [7] and personality correlates [8].

The number of studies investigating EEG activity during resting states as a potential biometric marker has increased, though the obtained results suggest that more efforts should be done to improve its efficacy in terms of correct recognition performance (CRR) and/or sample size, i.e. the number of subjects to recognize. A comprehensive survey of the different methods, protocols and achieved results can be found in [9].

As evidenced by this survey, the large part of the studies exploring EEG for biometric purposes has focused on the extraction of features from single electrodes. However, complementary information can be obtained from the temporal dependence between activities of different brain areas [10]. From a neuroscience perspective two brain regions that exhibit coherent or correlated activities are supposed to exchange information [11], [12] and this kind of communication represents nowadays a key element to understand the brain organization [13]. Many analytical tools are available to measure statistical interdependence between brain signals that are based on different mathematical principles (e.g. correlation, information theory, phase coherence, Granger-causality), implemented in the time and frequency domain, capturing either linear or nonlinear changes [14], [15]. These tools allow the estimation of the so-called functional brain connectivity [16].

Interestingly enough, we know that the way brain regions are functionally connected is not homogeneous, and that specific connectivity patterns emerge during wakeful resting state conditions [17]. Our hypothesis is that functional connectivity between EEG sensors could be a more robust feature for biometric recognition purpose, compared to EEG activity of channels considered separately. A previous study has tested, amongst others, time-domain connectivity measures between two frontal electrodes (Fp1 and Fp2) for the identification of 51 subjects [18]. The recognition accuracy, obtained separately with different classifiers, reached a maximum of CRR=31% for cross-correlation and CRR=24% for mutual information. In this regard, the large part of the studies using EEG for biometric purposes showed that the extraction of features describing the spectral content of the signals could give

better recognition performance [9]. Hence, frequency-domain connectivity measures could be more appropriate for detecting those putative distinctive features.

Changes of EEG amplitudes in the same subject and during the same condition can occur due to physiologic circadian rhythms [19], substance assumption [20], or different recording technical solutions [21]. In contrast to univariate measures, such as power spectrum estimates, spectral coherence is a simple bivariate connectivity method that is not sensitive to the amplitude changes of the EEG oscillations. In fact, two signals may have different amplitudes and/or phases, but high coherence occurs when this phase difference tends to remain constant [22]. Therefore, this property could play a critical role in increasing the overall classification performance in presence of large intra-subject EEG variability due to scale factors.

Another common issue in EEG-based biometric systems is the general tendency to perform classification from single elements, e.g. power spectra and/or functional connectivity [23], [24], [25],[18]. Less often the features space has been enriched by including information from a restricted number of a-priori selected elements [26], [27]. These parsimonious procedures appear certainly justified by possible implications on industrial research for smart EEG systems with few electrodes. However, such technical solution restricts the features space and consequently can affect the overall classification performance. Alternative methodological solutions integrating information from multiple elements can be beneficial with the aim of catching more robust and distinctive brain patterns, thus maximizing the recognition rates.

In this study we propose a fusion approach [28] to integrate at the match-score level the information obtained from the estimation of spectral coherence estimates.

The combined use of EEG spectral coherence and classification algorithms has been previously exploited in neuroscience to distinguish between healthy and diseased populations [29] or to determine changes between baseline and motor/cognitive tasks [30]. To the best of our knowledge, this is the first time that such a combined approach is also used for biometric purposes.

II. METHODS

A. Dataset and Preprocessing

Scalp EEG signals were gathered from the freely online database PhysioNet BCI [31]. The database consists of $N = 108$ healthy subjects recorded in two different baseline conditions, i.e. 1-minute EO resting state and 1-minute EC resting state. In each condition, subjects were comfortably seated on a reclining chair in a dimly lit room. During EO they were asked to avoid ocular blinks in order to reduce signal contamination. The EEG data were recorded with a 64-channel system (BCI2000 system [32]) with an original sampling rate of 160Hz. All the EEG signals are here referenced to the mean signal gathered from electrodes on the ear lobes. Data are subsequently downsampled to 100Hz after applying a proper anti-aliasing low-pass filter to restrict the available frequency range up to 50Hz. The electrode positions on the scalp follow the standard 10-10 montage. 5 electrodes are excluded and

only $N_{ch} = 56$ electrodes (see Figure 3) are retained for the subsequent analysis. These electrodes were selected because they constitute a montage common to different available datasets that we could use in future analysis.

For each subject and condition (EO, EC) the obtained EEG signals are segmented into $N_T = 6$ consecutive nonoverlapping epochs of 10 seconds. These epochs are considered as different observations of the same mental state and they are used to extract specific spectral features for the assessment of person recognition. In particular, we consider the two following methods, power spectral density and functional connectivity detailed in Sections II-B and II-C, respectively.

B. Power spectral density

Although parametric linear or non-linear EEG signal processing has been recently investigated for biometric purposes [33], [34], a non-parametric Fourier Transform-based spectral analysis is chosen in this study due to its obvious physical interpretation in terms of EEG rhythms. Specifically the power spectral density (PSD) of the EEG signals was extracted from each segmented epoch ($10s$) by computing the Welch's averaged modified periodogram. A sliding Hanning window of $1s$, with an overlap of $0.5s$, is applied to improve the estimation quality. The number of FFT points is set to 100 in order to have a PSD estimate with a frequency resolution of 1Hz (the frequency sampling is 100Hz). The resulting PSD for the electrode i, with $i = 1, \cdots, N_{ch}$, is a feature vector of $N_{FT} = 41$ elements characterizing the power of the EEG oscillations from 0 up to 40Hz. In the present study we consider a restricted range of frequency, namely $1 - 40$Hz. This choice covers the standard spectrum of physiologic EEG oscillations from low (Delta $1 - 3$Hz, Theta $4 - 7$Hz) to intermediate (Alpha $8 - 14$Hz) and high frequency bands (Beta $15 - 29$Hz, Gamma $30 - 40$Hz). Each segmented epoch is finally characterized by $N_E^{(PSD)} = N_{ch}$ feature vectors $\hat{\zeta}^{(PSD)}$ of $N_F = 40$ elements, where $N_{ch} = 56$ is the total number of electrodes.

C. Functional connectivity

In this study, functional connectivity is estimated by calculating the spectral coherence (COH) [35]. This method is frequently used due to its practical and intuitive interpretation. Spectral coherence quantifies the level of synchrony between two stationary signals at a specific frequency f. Given two signals obtained from channels i and j, the spectral coherence $COH_{i,j}(f)$ for a particular frequency f is computed as follows:

$$COH_{i,j}(f) = \frac{|S_{i,j}(f)|^2}{S_{i,i}(f) \cdot S_{j,j}(f)}. \quad (1)$$

where $S_{i,j}(f)$ is the cross-spectrum of the signals acquired from channels i and j, while $S_{i,i}(f)$ and $S_{j,j}(f)$ are the respective autospectra. By definition $COH_{i,j}(f)$ ranges between 0, which corresponds to no synchrony at the frequency f and 1, which corresponds to maximum synchrony at the frequency f. Here, $S_{i,j}(f), S_{i,i}(f)$ and $S_{j,j}(f)$ are computed by means of the Welch's averaged modified periodogram, with

same parameters used for the computation of the PSD (see Section II-B). In particular the use of 1s Hanning windows should improve the stationarity of the segmented EEG signals [36]. For each electrode pair, we consider a feature vector $\hat{\zeta}^{(COH)}$ consisting of $N_F = 40$ COH values ranging from $f = 1$Hz to $f = 40$Hz. The total number of electrodes N_{ch} being equal to 56, we have that $i = 1, \cdots, N_{ch} - 1$ and $j = i + 1, \cdots, N_{ch}$ and each segmented epoch ($10s$) is finally characterized by $N_E^{(COH)} = \frac{N_{ch} \cdot (N_{ch} - 1)}{2} = 1540$ features vectors of N_F elements.

D. Classifier

We use a classification approach to predict the class, namely the subject identity, to which the observed feature vector $\hat{\zeta}$ belongs. The model we use for the discriminant analysis assumes that the feature vectors $\hat{\zeta}$ form a Gaussian mixture distribution.

For this reason, before the classification, we apply a Fisher's Z transformation to the COH values in order to normalize their distributions [37]. A logarithmic transformation is instead applied to the PSD values [38].

A Mahalanobis distance-based classifier is then used to perform identification. This method requires the computation of the covariance matrix of the feature vectors of each class. Given the few observations for each subject (6 epochs) the covariance matrices cannot be robustly computed. Therefore we use a common procedure consisting in the simplification to equal covariance matrices [39]. Specifically, a pooled covariance matrix is obtained by merging the class-specific distributions of the feature vectors after removing their mean value. Notably, the normalizing transformation that we apply supports such approximation. A partition of the $N_T \times N$ normalized feature vectors extracted from the dataset is used to enroll the subjects and generate templates representing the class distributions.

A cross-validation framework is here considered to assess the recognition performance. In each cross-validation run, for each subject m, 5 epochs are used to generate the class distributions (i.e. enrollment phase), while the remaining epoch is employed to perform the identification (i.e. test phase). A number $N_r = 6$ of runs are provided, considering all possible partitions (leave-one-out framework). The Mahalanobis distances are computed between each observation m in the test dataset, and the class distributions n obtained in the enrolling, according to the formula:

$$d_{m,n} = (\hat{\zeta}_m - \mu_n)\Sigma^{-1}(\hat{\zeta}_m - \mu_n)^T \qquad (2)$$

with $m, n = 1, \cdots, N$, N being the number of classes (subjects), $\hat{\zeta}_m$ the observed feature vector from subject m, μ_n the mean vector for the class distribution n, and Σ the pooled covariance matrix.

We use the misclassification (or confusion) matrix $\mathbf{M}$ to evaluate the recognition performance. Each column of this matrix $N \times N$ represents the instances in a predicted subject identity (i.e. class), while each row represents the instances in an actual class. For a given subject m, the predicted subject identity $\hat{n}$ is obtained according to:

$$\hat{n} = \arg\min_n d_{m,n}. \qquad (3)$$

Eventually, for each run the correct recognition rate (CRR) is defined as the average over the diagonal of the resulting misclassification matrix $\mathbf{M}$:

$$CRR = \left(\frac{1}{N} \sum_{n=1}^{N} M[n,n] \right) \times 100. \qquad (4)$$

E. Match score fusion

Performance in terms of correct recognition percentage is computed as described in the previous Section for both the PSD based approach and the connectivity estimate based method, separately. We can observe that different elements, both channels and channel pairs, show to be distinctive for different groups of subjects correctly identified. Therefore we try to obtain complementary information considering activities of different brain areas, known not to be homogeneous, in order to improve overall performance. Through the fusion of single-element information we obtain patterns of brain activity, supposed to be a more robust characterization representative of brain organization of specific subjects. In this regard we perform a fusion at the match score level, considering the sum of scores related to different elements:

$$S_{m,n} = \sum_{e \in E} \frac{1}{d_{m,n}^e} \qquad (5)$$

where E is a selection of elements from the set of 56 channels for $\hat{\zeta}^{(PSD)}$, or from 1540 channel pairs when considering $\hat{\zeta}^{(COH)}$. We then compute the misclassification matrix $\mathbf{M}$ to evaluate recognition accuracy as described in Section II-D by maximizing $S_{m,n}$ with respect to n. We select the elements to consider in the match score fusion according to a forward-backward approach. Specifically only elements which improve accuracy are retained in the fusion. First, all the elements are sorted in a descending order of accuracy according to the single-element classification results. Starting from the first one, each single element is then added stepwise in the subset E to compute equation (5). If the inclusion of the i-th element improves the resulting accuracy then it is retained for the final fusion, otherwise it is removed (see Fig. 3). More details about the pseudo-code implementation of the match score fusion can be found in the Supplementary File 1).

Each step of the fusion algorithm is computed within a leave-on-out cross-validation framework, as discussed in Section II-D. Specifically, for each tested subset E of elements, related to a specific step of the fusion algorithm, $S_{m,n}$ is computed for each of the 6 partitions of the dataset. Then the CRRs related to the different partitions are averaged together to obtain the performance related to the particular step. If that performance represents an improvement compared to the previous step the related element is retained in E for the final fusion. This analysis is carried out separately for three cerebral zones, namely frontal (F), central (C), and parieto-occipital (P), in order to compare performance and distinctive activity patterns among them. These zones are selected according to
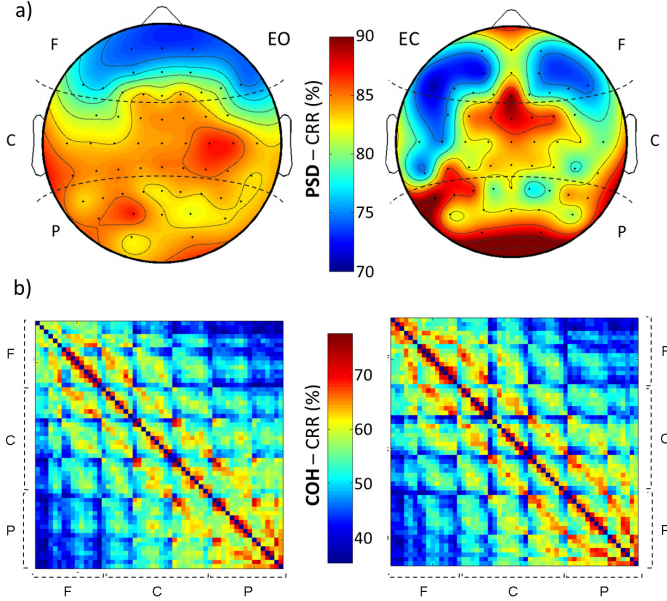
Fig. 1. Spatial distribution of CRR values obtained considering a) PSD features from single EEG channel and b) COH features from single channel pairs. In b) the elements of the adjacency matrices code all the possible EEG channel pairs. They are organized in order to highlight the connectivity within and between three zones: frontal (F), central (C), and parieto-occipital (P). The two analyzed conditions EO (on the left) and EC (on the right) are reported for each of the two investigated spectral features.

previous studies which showed an improvement of recognition accuracy spanning the scalp from the anterior part of the head to the posterior area [33], [25].

III. RESULTS AND DISCUSSION

In this section the results of the analysis performed for subject recognition based on EEG signals are reported and discussed. Resting-state conditions EO and EC are investigated separately and the related outcome is here compared for all the performed tests. Two different characterizations of the brain signals are considered as distinctive features to test within the provided biometric framework. In particular, after the preprocessing described in Section II-A, PSD and COH estimates are obtained as reported in Sections II-B and II-C. As previously pointed out, PSD measures the activity of single brain regions while COH rather measures their functional connectivity. Then, two different sets of feature vectors, $\hat{\zeta}^{(PSD)}$ and $\hat{\zeta}^{(COH)}$, are extracted according to the previously described methods. A classification based on Mahalanobis distance, detailed in Section II-D, is then carried out to evaluate the distinctiveness of the two considered feature vectors in all tested conditions, in terms of CRR.

A. Single-element classification

A preliminary test on distinctiveness related to each feature is reported in Fig. 1. The CRR values obtained within a cross-validation framework, as described in Section II-D, are shown in false colors. In particular the scalp maps shown in Fig. 1 (a) represent the spatial distribution of the CRR values obtained through single channel PSD features, in the

EO and EC conditions. The adjacency matrices shown in Fig. 1 (b) report the CRR values of the COH features for each channel pair. Given the $N_{ch} \times N_{ch}$ adjacency matrix **Adj**, each element $Adj_{i,j}$ represents the CRR obtained considering the COH between channels i, j as feature vector. According to this representation, the position of the EEG channels over the head is coded by the x and y axes of the adjacency matrix. The CRR scalp maps for the PSD features show that the most distinctive regions appear in the central part of the head (C) during EO (max CRR=86.91%),while the parieto-occipital zone (P) is more predominant during the EC condition (max CRR=90.49%). The better distinctiveness of the posterior areas during EC condition was already reported in previous EEG studies [25], [26], [33] and it is probably related to well-known physiological increase of the parieto-occipital Alpha power in such condition [40]. A possible explication for this evidence is that eyes-closed resting states interrupt the visual processing while enhancing endogenous and autonomic related brain activity [41], which reflects the influence of genetic factors [42]. For the CRR adjacency matrices in the EC condition the best discriminant channel pairs are mainly located in the parieto-occipital zone P (max CRR=78.5%). In the EO condition, the CRR values are generally lower compared to EC (max CRR=75.86%). In both conditions, short-range functional connectivity carries more distinctive information as can be observed by the tendency of the highest CRR values to stay close to the main diagonal of the **Adj** matrices.

B. Match-score fusion

To improve performance, a fusion of the elements at the match score level is obtained for each cerebral zone (F, C and P), within the same cross-validation framework described in Section II-E. The related improvements with respect to the single element approach are shown in Fig. 2. Here the two conditions EO and EC, and the two considered features PSD and COH, are compared. In general, a dramatic improvement with respect to the single element approach is obtained for each zone, condition and feature through the match score fusion approach. This is particularly true for the COH features, for which the fusion allows a perfect recognition rate $CRR = 100\%$ for the EC condition (in all the zones) and for the EO condition (in the frontal zone).

Fig. 3 shows the optimal combination of channel pairs in every zone for COH features (see Section II-E). Results are shown for the two conditions EO (a) and EC (b). The plots shown on the bottom part of the figure represent the steps of the match score fusion. Here, each highlighted symbol represents a subsequent improvement of the overall CRR, which leads to include the related channel pair in the final distinctive connectivity pattern represented in the upper part of the figure. It can be noticed that the maximum value of CRR is achieved more rapidly for the EC condition, as shown by the vertical lines in the plots of the bottom part of the figure. The resulting distinctive connectivity patterns consist mainly of short-range COH elements, a result which is in line with the previous outcome reported in the single-element

classification analysis. The topology of the more discriminant COH elements reveals a hemispheric symmetry with respect to the longitudinal line. In particular, the predominance of the frontal electrode pairs (line $F7 - F8$) can be observed in both the EO and EC conditions. Neurophysiological evidence shows that specific genetic factors can influence EEG frontal activity [43]. Thus the highly discriminant spectral coherence observed in this zone could in part reflect a subjective distinctiveness of brain functioning. We also report the involvement of temporo-parietal and dorsal centro-parietal electrodes of the central zone C. Brain regions near the temporo-parietal junction play a specific role in self-other distinction processes and in representing thoughts, beliefs, desires, and emotions [44], influenced by a combination of biological and environmental factors. A comprehensive analysis reporting the fusion steps for the spectral coherence features in all the conditions and zones is detailed in Table I, along with a description of the obtained identification accuracy and topology. A predominance of short-range connectivity characterizes the distinctive patterns for all the considered brain zones.

Notably, the inclusion of the long-range (i.e. inter-zone) connectivity in the fusion algorithm does not improve the recognition performance (Supplementary File 2).

The superiority of short-range over long-range connectivity could be partially imputed to volume condition effects, which are known to affect spectral coherence measurements [45]. Although removing those effects is important in general to estimate the real interaction between the cortical generators, this could not represent an issue in our study. In fact, volume conduction effects depend on the morphology and electrical conductibility of the subject's head structures. In this regard, any possible volume conduction contributions on the EEG signals could instead represent a relevant personal trait to be exploited for the biometric recognition. As a partial confirmation of our claim we reported that the recognition performance of the imaginary coherence (robust to volume conduction effects [45]) is significant lower than standard spectral coherence (Supplementary File 3).

To sum up, the results of the herein proposed analysis show that a perfect identification of 108 subjects ($CRR = 100\%$) can be obtained considering spectral coherence features within specific regions of the head, and fusing the respective information at the match score level. This result outperforms the state-of-the-art recognition performance obtained with EEG during resting states, notably a $CRR = 98.73\%$ for a dataset of 45 subjects [33] and a $CRR = 97.5\%$ for a dataset of 40 subjects [24].

C. Limitations and possible solution

The proposed approach presents methodological and technical limitations that should be taken into account in scenarios different from the presented experimental protocol. First, the spectral coherence requires EEG signals to be (quasi)stationary. Appropriate short time windows should be selected by testing the stationarity of the signals [46]. Alternatively different connectivity methods that don't require stationarity (e.g. wavelet-based) can be used [47]. Second, the
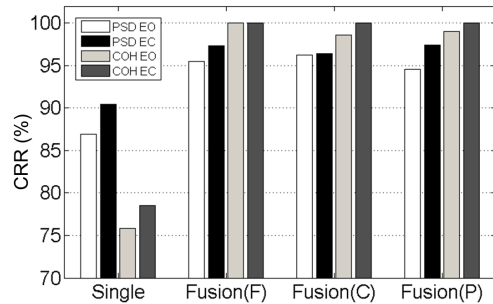

Fig. 2. Performances in terms of CRR (y-axis) obtained considering single-element classification versus match-score fusion in each cerebral zone (x-axis). The color of the bars codes the spectral feature and the condition according to the legend.

Mahalanobis distance-based classifier assumes that features are Gaussian distributed. Possible deviation from Gaussianity should be then compensated by applying appropriate data transformations [37] or using reduced polynomial regression-based classifiers (PRC) [48]. Third, the fusion approach implies that many EEG sensors need to be placed on the scalp. This affects the design of the biometric system and the time needed to establish a good skin-sensors electrical contact. Possible solutions can come from the technology development related to dry and miniaturized sensor helmets, or non-contact biosensors [49]. Finally, most of the computational time is spent during the off-line enrollment and definition of the fusion steps (around 20 min on a standard personal computer). Though it is not the aim of this study, we envisage that possible optimizations can be obtained by parallelizing the single-element ranking and the cross-validation runs.

IV. CONCLUSIONS

In the past few years there has been a growing interest in EEG-based biometric systems. Compared to other traits that are usually considered in biometrics (e.g. fingerprints, iris, voice, signatures, etc.), EEG activity presents two main advantages, among others: i) it's harder to steal and ii) it's a dynamic measure, thus allowing for constant recognition and mental state monitoring [4]. Despite such interest, classification performance decreases from maximum accuracy when the number of people to recognize becomes high, i.e. $N > 100$ [50], [51]. Possible causes rely on the methods that are commonly used to extract characteristic features from the EEG signals. Indeed, the majority of these methods only consider the activity of a single brain region without taking into account its dynamic relationship with other regions. It is worth pointing out that the human brain is known to be an interconnected system where different specialized areas continuously exchange information through stable synchronous connectivity patterns [10]. In the present study we propose to exploit such synchronous "communication" between different EEG sensors, under the hypothesis that this information could exhibit stronger intra-class invariant properties. Specifically, spectral coherence estimates within specific zones (i.e. frontal, central, parieto-occipital) are integrated according to a fusion at match score level [28] based on the sum rule.

	Eyes-Open											
F	72,74 F2-F4	91,43 F1-F3	94,55 F4-F6	97,2 F3-F5	97,82 F6-F8	99,06 F1-Fz	99,84 F5-F7	100 F2-Fz				
C	74.14 TP7-T7	91.28 CP5-TP7	92.99 C5-T7	95.33 T8-C6	96.26 FC2-FCz	97.04 C2-Cz	97.82 CP2-CPz	98.29 CP5-T7	98.44 TP8-CP6	98.6 CP6-T8		
P	75.86 P7-P5	91.59 PO4-PO8	93.92 O1-PO3	94.08 O1-PO7	94.39 P2-P4	95.79 PO7-P5	96.26 O1-O2	97.51 P2-Pz	98.29 P3-P5	98.75 P4-P6	98.91 POz-PO3	99.07 PO7-P1
	Eyes-Closed											
F	77.26 F2-F4	97.04 F3-F5	97.82 F1-F3	98.6 F5-F7	98.75 F6-F8	99.06 F4-F6	99.69 Fp2-Fpz	100 F2-F6				
C	72.43 TP7-T7	90.65 FC2-FCz	96.73 FC2-FC4	99.22 C6-T8	100 FC1-FC3							
P	78.5 PO3-O1	92.21 PO4-PO8	95.01 PO7-O1	98.13 PO3-PO7	98.29 P2-P4	98.44 PO7-P7	98.6 PO7-P5	99.06 P1-P3	99.69 O2-PO4	99.84 O2-POz	100 P4-Pz	

TABLE I

CRRs FOR COH FEATURES, OBTAINED THROUGH THE FUSION OF THE CHANNEL PAIRS REPORTED IN EACH ROW. EACH COLUMN REPRESENTS A STEP OF THE FUSION, AND THE RELATED ACCURACY ACHIEVED IS REPORTED TOGETHER WITH THE CHANNEL PAIR CONSIDERED IN THAT STEP (SEE SECTION II-E). RESULTS FOR EO, EC, AND THE THREE INVESTIGATED BRAIN ZONES ARE SHOWN.
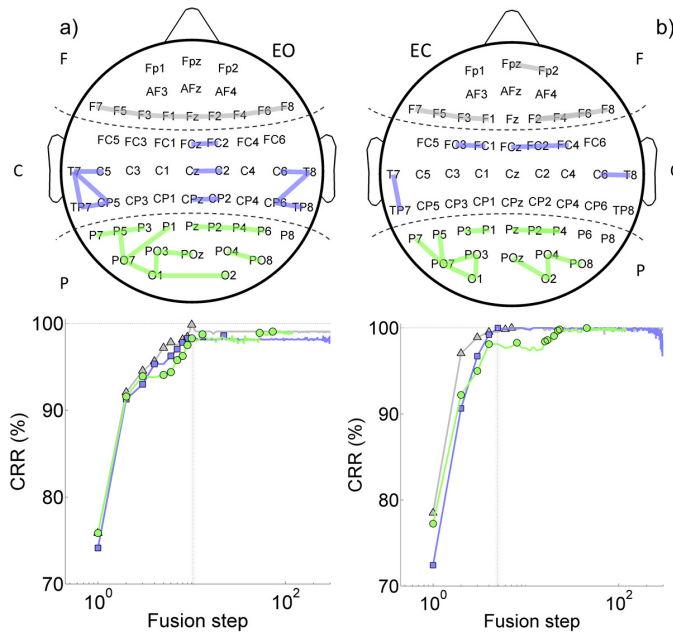

Fig. 3. Distinctive functional connectivity patterns in each cerebral zone (on the top) and related steps for the match score fusion selection (on the bottom). Results for the EO and EC to conditions are reported in a) and b) respectively. The color of each line in the bottom panels codes the CRR values obtained for different cerebral zones, according to the top panels. Symbol markers highlight the fusion steps that increased the overall CRR accuracy. Different symbols are used for different cerebral zones (F-triangles, C-circles, P-squares). X-axes are put into logarithmic scales for the sake of representation.

We test the proposed approach on a large number of subjects (N=108) having been recorded with a high-density EEG system with 56 electrodes available. Taken together, the obtained results indicate that the combined use of spectral coherence and fusion algorithms significantly improves the overall performance compared to existing standard techniques. Notably a perfect recognition can be achieved in both eyes-closed and eyes-open resting states by considering only 15 EEG sensors in the frontal region of the head. This also represents a technical advantage for future implementation of smart EEG-based biometric helmets.

Although connectivity-based approaches have not received much attention in this field, we suggest that they will probably turn out to be effective invariant features to further develop robust EEG-based user-recognition systems.

REFERENCES

[1] J. Berkhout and D. O. Walter, "Temporal stability and individual differences in the human EEG: An analysis of variance of spectral values," *IEEE Trans. Biomed. Eng.*, vol. 15, no. 3, pp. 165–168, 1968.

[2] H. Van Dis, M. Corner, R. Dapper, G. Hanewald, and K. H, "Individual differences in the human electroencephalogram during quiet wakefulness," *Electroenceph. and clin. neurophys.*, vol. 47, pp. 87–94, 1979.

[3] H. H. Stassen, "Computerized recognition of persons by EEG spectral patterns," *Electroenceph. and clin. neurophys.*, vol. 49, no. 1, pp. 190–194, 1980.

[4] P. Campisi, D. La Rocca, and G. Scarano, "EEG for automatic person recognition," *IEEE Computer*, vol. 45, no. 7, pp. 87–89, 2012.

[5] S. Marcel and J. del R. Millan, "Person authentication using brainwaves (EEG) and maximum a posteriori model adaptation," *IEEE Trans. Pattern Anal. Mach. Intell.*, vol. 29, no. 4, pp. 743–748, 2006.

[6] D. Mantini, M. G. Perrucci, C. D. Gratta, G. L. Romani, and M. Corbetta, "Electrophysiological signatures of resting state networks in the human brain," *Proc. Natl. Acad. Sci. U.S.A.*, vol. 104, no. 32, pp. 13 170–13 175, Aug 2007.

[7] F. Vogel and E. Schalt, "The electroencephalogram (EEG) as a research tool in human behavior genetics: Psychological examinations in healthy males with various inherited EEG variants," *Hum. Genet.*, vol. 47, pp. 81–111, 1979.

[8] A. J. Tomarken, R. J. Davidson, R. E. Wheeler, and L. Kinney, "Psychometric properties of resting anterior EEG asymmetry: Temporal stability and internal consistency," *Psychophysiology*, vol. 29, no. 5, pp. 576–592, 1992.

[9] P. Campisi and D. La Rocca, "Brain waves for automatic biometric based user recognition," *IEEE Trans. Inf. Forensics Security*, 2014, in press.

[10] F. Varela, J.-P. Lachaux, E. Rodriguez, and J. Martinerie, "The brainweb: Phase synchronization and large-scale integration," *Nat. Rev. Neurosci.*, vol. 2, no. 4, pp. 229–239, Apr. 2001.

[11] T. Akam and D. M. Kullmann, "Oscillations and filtering networks support flexible routing of information," *Neuron*, vol. 67, no. 2, pp. 308–320, 2010.

[12] L. Astolfi, F. Cincotti, D. Mattia, S. Salinari, C. Babiloni, A. Basilisco, P. M. Rossini, L. Ding, Y. Ni, B. He *et al.*, "Estimation of the effective and functional human cortical connectivity with structural equation modeling and directed transfer function applied to high-resolution eeg," *J. Magn. Reson. Imaging*, vol. 22, no. 10, pp. 1457–1470, 2004.

[13] B. He, L. Yang, C. Wilke, and H. Yuan, "Electrophysiological imaging of brain activity and connectivitychallenges and opportunities," *IEEE Trans. Biomed. Eng.*, vol. 58, no. 7, pp. 1918–1931, 2011.

[14] O. David, D. Cosmelli, and K. J. Friston, "Evaluation of different measures of functional connectivity using a neural mass model," *Neuroimage*, vol. 21, no. 2, pp. 659–673, 2004.

[15] M. Billinger, C. Brunner, and G. R. Mller-Putz, "Single-trial connectivity estimation for classification of motor imagery data," *Journal of neural engineering*, vol. 10, no. 4, p. 046006, Aug. 2013, PMID: 23751454.

[16] K. J. Friston, "Functional and effective connectivity: a review," *Brain connect.*, vol. 1, no. 1, pp. 13–36, 2011.

[17] H. Laufs, K. Krakow, P. Sterzer, E. Eger, A. Beyerle, A. Salek-Haddadi, and A. Kleinschmidt, "Electroencephalographic signatures of attentional and cognitive default modes in spontaneous brain activity fluctuations at rest," *Proc. Natl. Acad. Sci. U.S.A.*, vol. 100, no. 19, pp. 11 053–11 058, 2003.

[18] A. Riera, A. Soria-Frisch, M. Caparrini, C. Grau, and G. Ruffini, "Unobtrusive biometric system based on electroencephalogram analysis," *EURASIP J. Adv. Signal Process*, 2008.

[19] D. Aeschbach, J. R. Matthews, T. T. Postolache, M. A. Jackson, H. A. Giesen, and T. A. Wehr, "Two circadian rhythms in the human electroencephalogram during wakefulness," *Am. J. Physiol. Regul. Integr. Comp. Physiol.*, vol. 277, no. 6, pp. R1771–R1779, 1999.

[20] T. M. Sokhadze, R. L. Cannon, and D. L. Trudeau, "Eeg biofeedback as a treatment for substance use disorders: review, rating of efficacy and recommendations for further research," *J. Neurother.*, vol. 12, no. 1, pp. 5–43, 2008.

[21] T. C. Ferree, P. Luu, G. S. Russell, and D. M. Tucker, "Scalp electrode impedance, infection risk, and eeg data quality," *Clin. Neurophysiol.*, vol. 112, no. 3, pp. 536–544, 2001.

[22] P. L. Nunez, *Electric fields of the brain: the neurophysics of EEG*. Oxford University Press, 2006.

[23] M. Poulos, M. Rangoussi, and N. Alexandris, "Neural network based person identification using EEG features," in *Proc. IEEE Int. Conf. Acoust. Speech Signal Process.*, vol. 2, 1999, pp. 1117–1120.

[24] F. Su, H. Zhou, Z. Feng, and J. Ma, "A biometric-based covert warning system using EEG," in *Proc. 5th IAPR Int. Conf. on Biometrics (ICB)*, 2012, pp. 342–347.

[25] F. De Vico Fallani, G. Vecchiato, J. Toppi, L. Astolfi, and F. Babiloni, "Subject identification through standard eeg signals during resting states," in *Proc. IEEE Int. Conf. Eng. Med. Biol. Soc.*, 2011, pp. 2331–2333.

[26] P. Campisi, G. Scarano, F. Babiloni, F. De Vico Fallani, S. Colonnese, E. Maiorana, and F. L., "Brain waves based user recognition using the eyes closed resting conditions protocol," in *IEEE WIFS*, Nov. 2011, pp. 1–6.

[27] D. La Rocca, P. Campisi, and J. Sole-Casals, "Eeg based user recognition using bump modelling," in *Proc. Int. Conf. BIOSIG*, 2013, pp. 1–12.

[28] A. A. Ross, K. Nandakumar, and A. K. Jain, *Handbook of multibiometrics*. Springer, 2006.

[29] F. H. Duffy and H. Als, "A stable pattern of EEG spectral coherence distinguishes children with autism from neuro-typical controls - a large case control study," *BMC Med.*, vol. 10, no. 1, p. 64, 2012.

[30] D. J. Krusienski, D. J. McFarland, and J. R. Wolpaw, "Value of amplitude, phase, and coherence features for a sensorimotor rhythm-based brain-computer interface," *Brain Res. Bull.*, vol. 87, no. 1, pp. 130–134, Jan. 2012.

[31] Database physionet bci. [Online]. Available: http://www.physionet.org/pn4/eegmmidb/

[32] Bci2000 system. [Online]. Available: http://www.bci2000.org

[33] D. La Rocca, P. Campisi, and G. Scarano, "EEG biometrics for individual recognition in resting state with closed eyes," in *Proc. Int. Conf. BIOSIG*, 2012, pp. 1–12.

[34] M. Poulos, M. Rangoussi, N. Alexandris, and A. Evangelou, "Person identification from the eeg using nonlinear signal classification," *Methods Inf Med.*, vol. 41, no. 1, pp. 64–75, 2002.

[35] F. G. Andres and C. Gerloff, "Coherence of sequential movements and motor learning," *J. Clin. Neurophysiol.*, vol. 16, no. 6, p. 520, 1999.

[36] A. A. Fingelkurts and A. A. Fingelkurts, "Making complexity simpler: multivariability and metastability in the brain," *Int. J. Neurosci.*, vol. 114, no. 7, pp. 843–862, 2004.

[37] A. Amjad, D. Halliday, J. Rosenberg, and B. Conway, "An extended difference of coherence test for comparing and combining several independent coherence estimates: theory and application to the study of motor units and physiological tremor," *J. Neurosci. Methods*, vol. 73, no. 1, pp. 69–79, 1997.

[38] T. Gasser, P. Bächer, and J. Möcks, "Transformations towards the normal distribution of broad band spectral parameters of the eeg," *Electroencephalogr. Clin. Neurophysiol.*, vol. 53, no. 1, pp. 119–124, 1982.

[39] J. Schürmann, *Pattern classification: a unified view of statistical and neural approaches*, ser. A Wiley-Interscience publication. John Wiley & Sons, 1996.

[40] E. Niedermeyer, *The Normal EEG of the Waking Adult*. Lippincott Williams & Wilkins, 2005, ch. Electroencephalography: Basic princ., clin. app., and related fields, p. 167.

[41] R. Barry, A. Clarke, S. Johnstone, C. Magee, and J. Rushby, "EEG differences between eyes-closed and eyes-open resting conditions," *Clin. Neurophysiol.*, vol. 118, no. 12, pp. 2765–2773, 2007.

[42] S. Bodenmann, T. Rusterholz, R. Dürr, C. Stoll, V. Bachmann, E. Geissler, K. Jaggi-Schwarz, and H.-P. Landolt, "The functional val158met polymorphism of comt predicts interindividual differences in brain α oscillations in young men," *J. Neurosci.*, vol. 29, no. 35, pp. 10 855–10 862, 2009.

[43] B. P. Zietsch, J. L. Hansen, N. K. Hansell, G. M. Geffen, N. G. Martin, and M. J. Wright, "Common and specific genetic influences on EEG power bands delta, theta, alpha, and beta," *Biol. Psychol.*, vol. 75, no. 2, pp. 154 – 164, 2007. [Online]. Available: http://www.sciencedirect.com/science/article/pii/S0301051107000099

[44] R. Saxe and N. Kanwisher, "People thinking about thinking people: the role of the temporo-parietal junction in theory of mind," *Neuroimage*, vol. 19, no. 4, pp. 1835–1842, 2003.

[45] G. Nolte, O. Bai, L. Wheaton, Z. Mari, S. Vorbach, and M. Hallett, "Identifying true brain interaction from eeg data using the imaginary part of coherency," *Clin. Neurophysiol.*, vol. 115, no. 10, pp. 2292–2307, 2004.

[46] D. Kwiatkowski, P. C. B. Phillips, P. Schmidt, and Y. Shin, "Testing the null hypothesis of stationarity against the alternative of a unit root," *J. Econometrics*, vol. 54, no. 1-3, pp. 159–178, 1992.

[47] M. Le Van Quyen, J. Foucher, J.-P. Lachaux, E. Rodriguez, A. Lutz, J. Martinerie, and F. J. Varela, "Comparison of hilbert transform and wavelet methods for the analysis of neuronal synchrony," *J. Neurosci. Methods*, vol. 111, no. 2, pp. 83–98, 2001.

[48] G. Scarano, L. Forastiere, S. Colonnese, and S. Rinauro, "Reduced polynomial classifier using within-class standardizing transform," in *Communications Control and Signal Processing (ISCCSP), 2012 5th International Symposium on*. IEEE, 2012, pp. 1–4.

[49] Y. M. Chi, T.-P. Jung, and G. Cauwenberghs, "Dry-contact and non-contact biopotential electrodes: methodological review," *Biomedical Engineering, IEEE Reviews in*, vol. 3, pp. 106–119, 2010.

[50] K. Brigham and B. V. Kumar, "Subject identification from electroencephalogram (EEG) signals during imagined speech," in *Proc. IEEE 4th Int. Conf. BTAS*, 2010, pp. 1–8.

[51] R. Palaniappan and D. Mandic, "Biometrics from brain electrical activity: A machine learning approach," *IEEE Trans. Pattern Anal. Mach. Intell.*, vol. 29, no. 4, pp. 738–742, 2007.